4D in vivo ultrafast ultrasound imaging using a row-column addressed matrix and coherently-compounded orthogonal plane waves

M Flesch, M Pernot, J Provost, G Ferin, A Nguyen-Dinh, M Tanter, Thomas Deffieux

4D in-vivo ultrafast ultrasound imaging using a row-column addressed matrix and coherently-compounded orthogonal plane waves

4D in-vivo Ultrafast Ultrasound Imaging using a Row-Column Addressed matrix and Coherently-Compounded Orthogonal Plane Waves

M Flesch[1,2], M Pernot[1], J Provost[1], G Ferin[2], A Nguyen-Dinh[2], M Tanter[1] and T Deffieux[1]

1 - Institut Langevin, ESPCI Paris, PSL Research University, CNRS UMR7587, INSERM U979, Paris VII, France, www.institut-langevin.espci.fr

2 - Vermon, France, www.vermon.com

m.flesch@vermon.com

Abstract

4D ultrafast ultrasound imaging was recently shown using a 2D matrix (i.e., fully populated) connected to a 1024-channel ultrafast ultrasound scanner. In this study, we investigate the Row-Column Addressing (RCA) matrix approach, which allows a reduction of independent channels from N x N to N + N, with a dedicated beamforming strategy for ultrafast ultrasound imaging based on the coherent compounding of Orthogonal Plane Wave (OPW). OPW is based on coherent compounding of plane wave transmissions in one direction with receive beamforming along the orthogonal direction and its orthogonal companion sequence. Such coherent recombination of complementary orthogonal sequences leads to virtual transmit focusing in both directions which results into a final isotropic Point Spread Function (PSF).

In this study, a 32 x 32 2D matrix array probe (1024 channels), centered at 5 MHz was considered. An RCA array, of same footprint with 32 + 32 elements (64 channels), was emulated by summing the elements either along a line or a column in software prior to beamforming. This approach allowed for the direct comparison of the 32 + 32 RCA scheme to the optimal fully sampled 32 x 32 2D matrix configuration, which served as the gold standard.

This approach was first studied through PSF simulations and then validated experimentally on a phantom consisting of anechoic cysts and echogenic wires. The Contrast-to-Noise Ratio (CNR) and the lateral resolution of the RCA approach were found to be approximately equal to half (in decibel) and twice the values, respectively, obtained when using the 2D matrix approach. Results in a Doppler phantom and the human humeral artery in vivo confirmed that ultrafast Doppler imaging can be achieved with reduced performances when compared against the equivalent 2D matrix. Volumetric anatomic Doppler rendering and voxel-based pulsed Doppler quantification are presented as well. OPW compound imaging using emulated RCA matrix can achieve a power Doppler with sufficient contrast to recover the vein shape and provides an accurate Doppler spectrum.

Introduction

The concept of ultrafast ultrasound imaging with plane waves has been introduced more than 15 years ago in order to map, at several thousand of images per second, the rapid transient events occurring in the human body (Tanter & Fink 2014). Recent progress of ultrafast imaging has allowed the development of novel modalities such as shear wave elastography (Bercoff et al. 2008), ultrasensitive Doppler imaging and functional ultrasound imaging (Mace et al. 2013), to name a few.

Recently, 4D ultrafast imaging was developed and experimentally applied to ultrafast Doppler and Shear-wave imaging *in vivo* in several organs (Provost et al. 2014) (Gennisson et al. 2015) (Provost et al. 2015), including the heart and the breast, using a 4D ultrafast ultrasound imaging research platform with 1024 active channels and a 32 x 32 matrix probe (Ratsimandresey et al. 2002) in contrast with the 128 channels used typically on regular commercial 2D scanner. Electronics with such a large channel count provide a high flexibility and as such are ideal for research applications (Jensen et al. 2013), but their complexities limit clinical and commercial implementations.

Large fully sampled 2D matrix arrays transducers are also difficult to manufacture because of the high density of elements to individually connect, which require complex and expensive manufacturing processes, especially at high frequency where the inter-element pitch is smaller. Moreover, the high electrical impedance and low sensitivity of the small elements compromise matrix array performances. Finally, the large coaxial cable count required to connect all individual elements to electronic channels strongly limits the ergonomics and the portability of the probe. On the scanner side, synchronizing electronic boards with more than 1024 independent channels remains prohibitive in terms of development and production costs. Scaling to an even higher number of elements such as 64 x 64 or 128 x 128 is currently out of reach outside of dedicated research platforms.

Consequently, the road for 4D ultrafast imaging toward the clinic may still rely on alternative methods to efficiently reduce the thousands individual probe elements into a more manageable number of system channels (regularly 128 channels), while still maintaining high spatial and temporal resolution.

Alternative methods have been extensively developed for volumetric ultrasound imaging to reduce the number of electronic channels, including mechanical scanning, 2D matrix with integrated analog front-end electronics such as multiplexers (Hara et al. 2005) or µ-beamformers (Savord & Solomon 2003). However, these approaches provide relatively low volume rate and are not compatible with ultrafast imaging.

Sparse arrays have been proposed as a solution to maintain a reasonable amount of output channels. Sparse arrays are made of a limited number of elements that are generally randomly positioned over the array footprint (Davidsen & Smith 1993). However, this geometry with large spacing between elements is not straightforward for the transmission of plane waves or diverging waves.

In this paper, we study another configuration of under-sampled arrays, i.e., the RCA matrix, originally proposed in 2003 (Morton & Lockwood 2003). RCA matrices are composed of two sets of orthogonal vertical and horizontal overlapping transducers which effectively reduces the number of elements from N x N to N + N individual channels, as shown in figure 1, and ensure compatibility with commercial scanners at the cost of a reduced image quality.

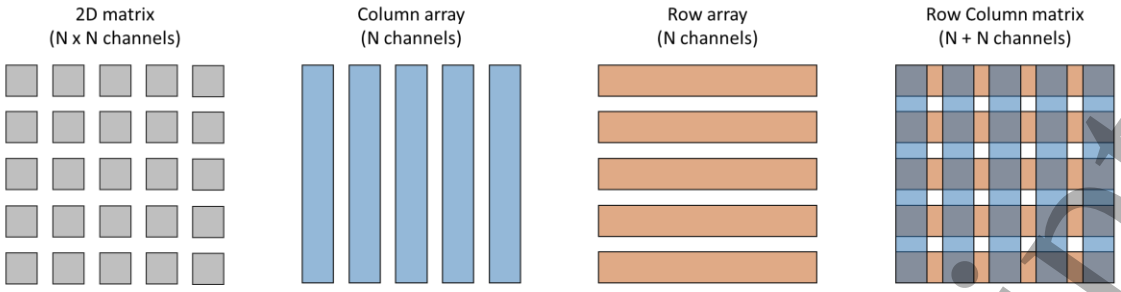

Figure 1 : RCA matrix basic principle

Compared to sparse arrays, RCA matrices have two advantages: a much larger active surface and a geometry that is inherently adapted to plane wave transmissions, which make them a good candidate for ultrafast plane wave imaging using coherent compounding.

Recently, the fabrication and assessment of RCA matrices using novel approaches based on various technologies such as lead zirconate titanate (PZT) (Seo & Yen 2009), polyvinylidene fluoride layer (PVdF) (Yen et al. 2009), or capacitive micromachined ultrasonic transducers (cMUT) (Logan et al. 2009) have been the object of active research.

Moreover, RCA matrices have been leveraged in various imaging sequences such as conventional beam focusing (Morton & Lockwood 2003), synthetic aperture techniques (Rasmussen et al. 2015), vector Doppler imaging (Lehrmann et al. 2015), or plane wave emissions with multiplexed reception (Chen et al. 2014), but, to our knowledge, no *in vivo* study on the full volumetric Doppler imaging capability of the RCA scheme has been conducted or compared against a 2D matrix.

In this work, we introduce an OPW compounding strategy dedicated to RCA matrices and have evaluated its performance for 4D ultrafast Doppler imaging against a 2D matrix approach. We first evaluate OPW in terms of PSF in simulation and then proceed to demonstrate its feasibility in phantoms and in a healthy volunteer.

1. Materials & Methods

1.1. OPW compounding

Ultrafast ultrasound imaging using a 1D or 2D array relies both on the parallel receive of channels data and the decomposition of the transmit focusing on an efficient and versatile basis with coherent compounding. A typical emission basis is a set of tilted plane waves or diverging waves, which allows a good repartition of the propagated energy in the medium and a good decorrelation between emissions. The method benefits from dynamic focusing both in transmit and receive and thus converges to quality of synthetic aperture imaging. The key point of this approach is the flexibility between image quality and frame rate, which can be adjusted by varying the number of emissions compounded for each image.

In the case of a RCA matrix, the focusing in transmit or receive can only be performed using a cylindrical law due to the geometry of the array. To achieve spatial separation, it is thus necessary to use complementary transmit and receive focusing: typically a cylindrical transmit focusing with the rows and an orthogonal cylindrical receive focusing with the columns or vice versa. However, it is still possible to decompose the cylindrical transmit focusing on a more efficient basis such as tilted plane waves and to use parallel receive with conventional delay and sum beamforming for dynamic receive focusing. Regarding the transmit, the emissions basis has to be adapted to the constraints of the RCA matrix which obviously rules out spherically diverging or converging waves or plane waves with random directions. Herein, we propose to use horizontally and vertically tilted plane waves, which can easily be transmitted using the RCA array by applying transmit delays rows or columns.

Contrary to the synthetic aperture approach, since the transmit focusing is not perfect but an approximation of the cylindrical focusing, the symmetry between emission and reception is broken and transmitting with rows then receiving with columns or transmitting with columns then receiving with rows lead to different results. As such, in order to enforce isotropy of the PSF at least in the two main axis we propose to coherently combine both sequences in a scheme we denote HV+VH where HV stands for Horizontal emission with Vertical reception and VH for Vertical emission with Horizontal reception as shown in figure 2.

Such dual scheme yields to a number of Na emissions where Na is the total number of angles of plane waves for both directions. While a lower image quality is to be expected when compared against focused or synthetic aperture approaches, it has the benefit of allowing for high volume rates. Table 1 summarizes the number of emissions required by the aforementioned approaches.

	2D Matrix (N x N channels)			RCA Matrix (N + N channels)		
Type of sequence	Focused	Synthetic aperture	Diverging waves compounding	Focused	Synthetic aperture	OPW compounding
Number of transmits	N2	N2	Na << N2	N	N	Na < N

Table 1 : Principal imaging schemes for 2D Matrices and RCA Matrices. Where N is the number of elements along a dimension of the array and Na is the number of plane or diverging waves used.

In figure 2, the plane wave compounding strategies for 2D matrix and RCA matrix are illustrated with their respective PSF. Figure 2a shows the regular compounding strategy dedicated to ultrafast ultrasound imaging using 2D matrices that is based on our previous work (Provost et al. 2014). Figure 2b shows the proposed OPW strategy dedicated to ultrafast imaging using RCA matrices.

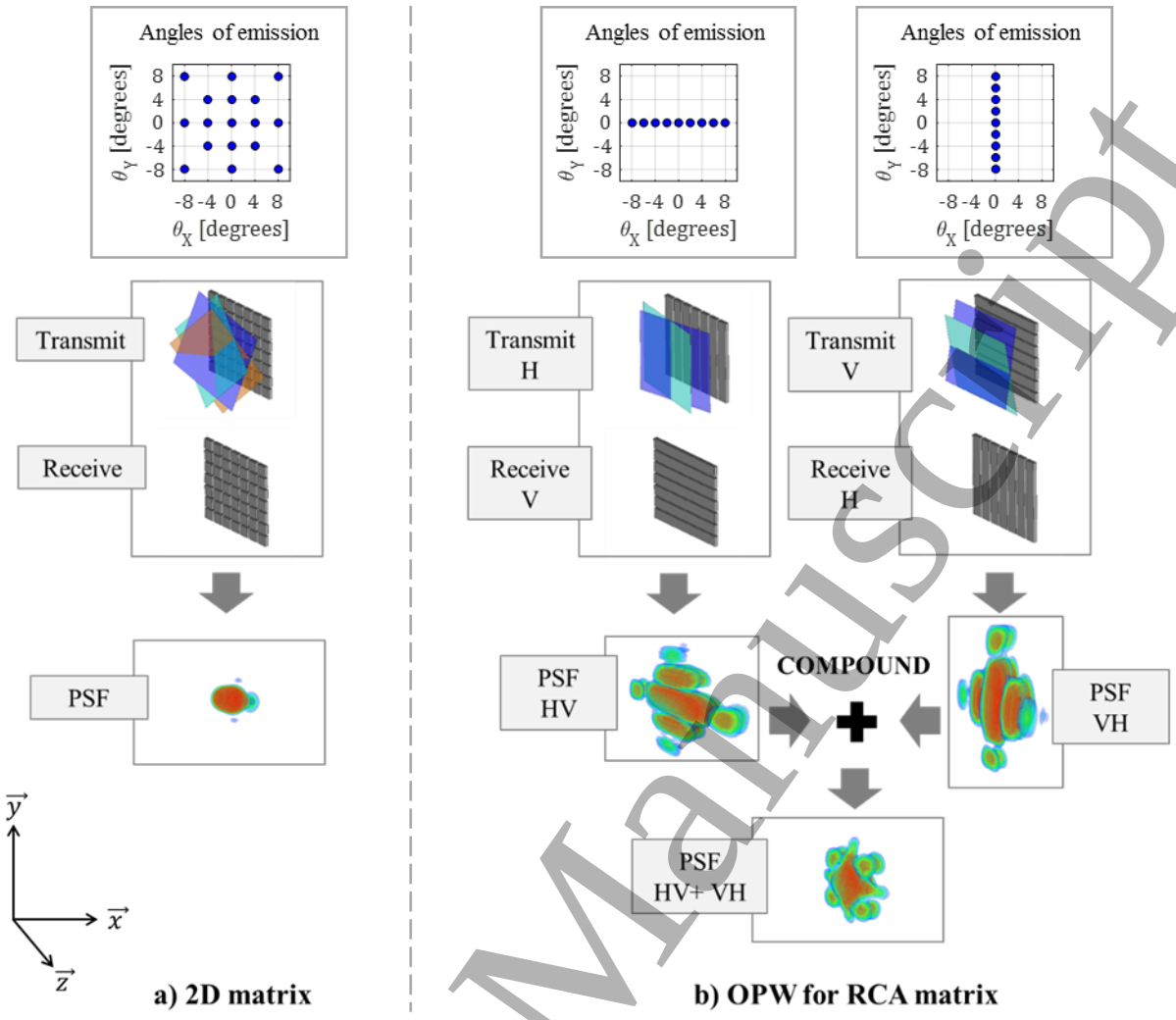

Figure 2 : Plane wave compounding for 2D matrix a) and OPW compounding for RCA matrix b)

The HV PSF and VH PSF have an extended shape in the transmit focusing direction. This is mainly caused by the partial focusing in transmit relying on the compounding of a few plane waves. As noted earlier, to reduce this effect, we choose to compound the volume obtained for the two complementary sequences since their respective PSF are rotated at 90 degrees. The OPW compounding strategy relies on summing the HV PSF and the VH PSF side lobes that are not located in the same location in space and thus reducing the final side lobe levels on the combined (HV + VH) PSF.

Since the aim of this study is to perform 4D ultrafast Doppler imaging, we compared the performances of the RCA matrix approach against the performances of the 2D matrix approach for a fixed frame rate, i.e., and equal number of emissions figure 2.

As described above, RCA matrices can only transmit a plane wave tilted either along the X or the Y axis, unlike the 2D matrix. Hence, an identical number of tilted planes were distributed uniformly in the $[\theta_X, \theta_Y]$ space for the 2D matrix, whereas tilted planes were distributed only in the $[\theta_X, 0] \cup [0, \theta_Y]$ space in the case of the RCA matrix. The same angular range was used in both cases.

1.2. PSF simulation

The numerical study focuses on the two configurations stated above: a 32 x 32 2D matrix and a 32 + 32 RCA matrix. The RF (Radio Frequency) signals were generated using Field II (Jensen & Svendsen 1992). A dedicated delay-and-sum beamforming was applied on the RF signals to compute the Bscan volume of a unique scatterer. The scatterer was centered in front of the transducer at a depth equal to 1.5 times the transducer aperture (i.e., 14 mm). A Hanning apodization with a F-number of 1.5 was used in reception. The excitation of the transducer consisted of 2 periods of a 5 MHz sinusoid with Hanning weighting. As described in figure 2a, 17 tilted plane waves were equally distributed within an angular range of -8 to +8 degrees for the 2D and the RCA matrix, corresponding to a volume rate of 2.9 KHz and transmitted in sequential order by increasing angle.

1.3. Ultrasound scanner and probe

The experimental setup was based on a customized, programmable, 1024-channel ultrasound system (Provost et al. 2014) used to drive a PZT piezocomposite based 32 x 32 2D matrix array transducer centered at 5 MHz with a 300-µm pitch (Vermon, Tours, France).The system was composed of four 256-transmit/128-receive-channels units initially designed for 2D imaging on an Aixplorer system (Supersonic Imagine, Aix-en-Provence, France), assembled into a 1024-channel device with synchronized boards. The total channel count was thus 1024 in transmit and 512 in receive. Because the receive channels were multiplexed to 1 of 2 transducer elements, each emission was repeated twice to synthetize a total of 1024 receive channels.

1.4. Emulated RCA matrix

Figure 3 shows the basic principle of the RCA emulation: in transmission, the probe is steered by flat delays along a line or a column whereas in reception, the RF signals are summed across the line or the column in post treatment. This approach allows for the direct comparison of the 32 + 32 RCA scheme to the optimal 32 x 32 2D matrix configuration, with all other parameters kept constant (transducer aperture, central frequency, bandwidth, field of view, etc.). The hypothesis that a line of RCA matrix share the same acoustic properties that a set of aligned elements on 2D matrix could be justified in term of active area. Indeed the kerf (distance between transducer elements) is significantly smaller than the pitch.

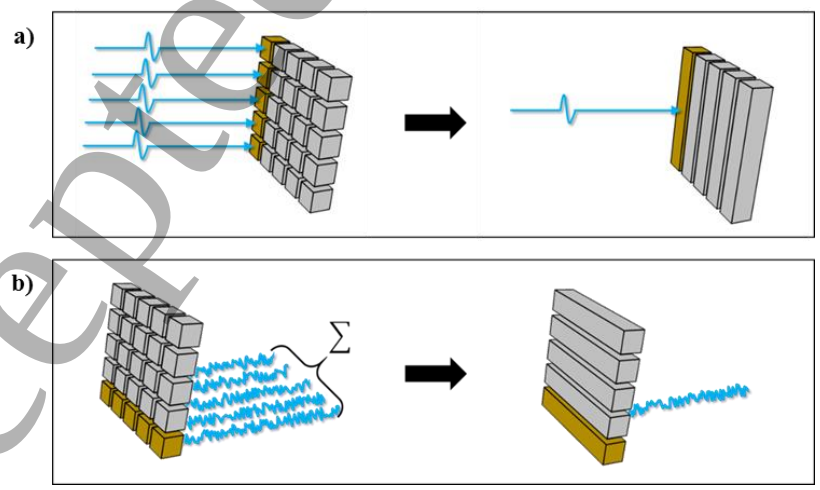

Figure 3 : A 2D matrix emulated in a RCA column for transmit a) and a 2D matrix emulated in a RCA line for receive b)

1.5. *Beamforming and power Doppler processing*

Figure 4 illustrates the HV sequence: in transmit, a horizontal linear array emits a plane wave tilted by an angle of θ while a vertical linear array receives. Only 5 rows and 5 columns of the 32+32 RCA matrix are depicted for readability. We presented here the calculation of the delay associated to a voxel v with coordinate (x, y, z) for a regular, delay-and-sum beamforming.

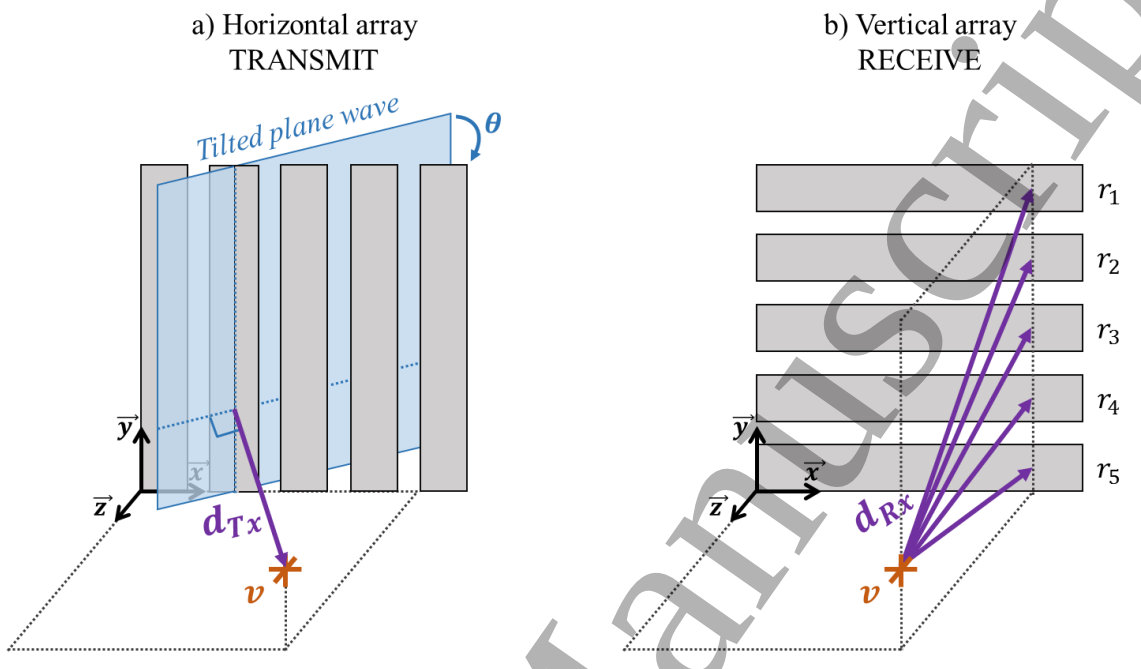

Figure 4 : Forward a) and backward b) distances illustration for an HV sequence on a RCA matrix

The forward distance d_{Tx} calculation is based on the regular plane wave beamforming algorithm. It corresponds to the projection of the voxel v on the tilted plane wave as shown in figure 4a (Montaldo et al. 2009).

$$d_{Tx}(x, z, \theta) = [z \cdot cos(\theta) + x \cdot sin(\theta)]$$

The backpropagation distance, d_{Rx} was calculated from the projection of the voxel v onto each row element r_i (figure 4b) due to the long elements used in the RCA configuration (Rasmussen et al. 2015):

$$d_{Rx}(y, z, r_i) = \sqrt{z^2 + (y - r_i)^2}$$

The delays τ are then given by:

$$\tau(x, y, z, \theta, r_i) = \frac{1}{c} \cdot d_{Tx}(x, z, \theta) + \frac{1}{c} \cdot d_{Rx}(y, z, r_i),$$

where c is the speed of sound.

A beamformed volume was computed by repeating the delay and sum algorithm for several voxels. A compounded beamformed volume was computed by coherent summation of the beamformed volumes obtained for each titled plane wave. The process was then applied to both the VH and the HV sequences (figure 2).

Full-view, ultrafast Doppler imaging volumes were obtained by first removing clutter from the beamformed baseband data using multidimensional spatiotemporal filtering (Demené et al. 2015), applied in four dimensions (i.e., 3D space + time) (Provost et al., 2015). This technique consists in eliminating clutter signal by removing the low-frequency principal components of the temporal

realizations of each voxel. Power Doppler volumes were then obtained by integrating the energy of the clutter-free baseband signal over time. Voxel-wise pulsed Doppler was obtained by calculating the short-time Fourier transform of the clutter-free baseband signals in the temporal direction using overlapping windows of 16 ms.

All beamforming and Doppler processing were performed on graphical processing units and were coded using CUDA C language within a Matlab (2016a, The MathWorks Inc., Natick, MA, USA) interface. A typical acquisition including all data transfers and calculations such as volume beamforming and Doppler processing required a total of fewer than 5 minutes. Calculation times are dependent on imaging depth and sampling.

1.6. In vitro 4D ultrafast CNR and resolution

The experiment was conducted on a commercial phantom (ATS Inc., Small Parts Ultrasound Phantom Model 551, Bridgeport, CT. USA), consisting of anechoic cysts (cylinders with a radius equal to 2 mm) and echogenic wires (0.05 mm in diameter). CNR and resolution were quantified for both 2D and the RCA matrix. CNR was defined as the ratio between energy outside and inside the anechoic cyst.

$$CNR = 10 \cdot \log_{10} \frac{\sum_{x,y,z \,\epsilon\, D_{out}} |IQ(x,y,z)|^2}{\sum_{x,y,z \,\epsilon\, D_{in}} |IQ(x,y,z)|^2} \quad (1)$$

The denominator represents the anechoic inclusion signal and is computed as the mean of the voxels include within the cyst shape. The numerator represents the background signal. It is computed as the mean of the voxels outside the cyst (Tiran et al. 2015). The lateral resolution was defined as the lateral width of the main peak at -6 dB. A Hanning apodization with a F-number of 1.5 was fixed in reception.

The excitation of the transducer consisted of 2 periods of a 5-MHz sinusoid. The final volumes was obtained by compounding either 1, 4, 16, or 36 tilted plane waves equally distributed within an angular range of -16 to +16 degrees for the 2D and the RCA matrix and transmitted in sequential order by increasing angle figure 5. The pulse repetition frequency was equal to 16 kHz.

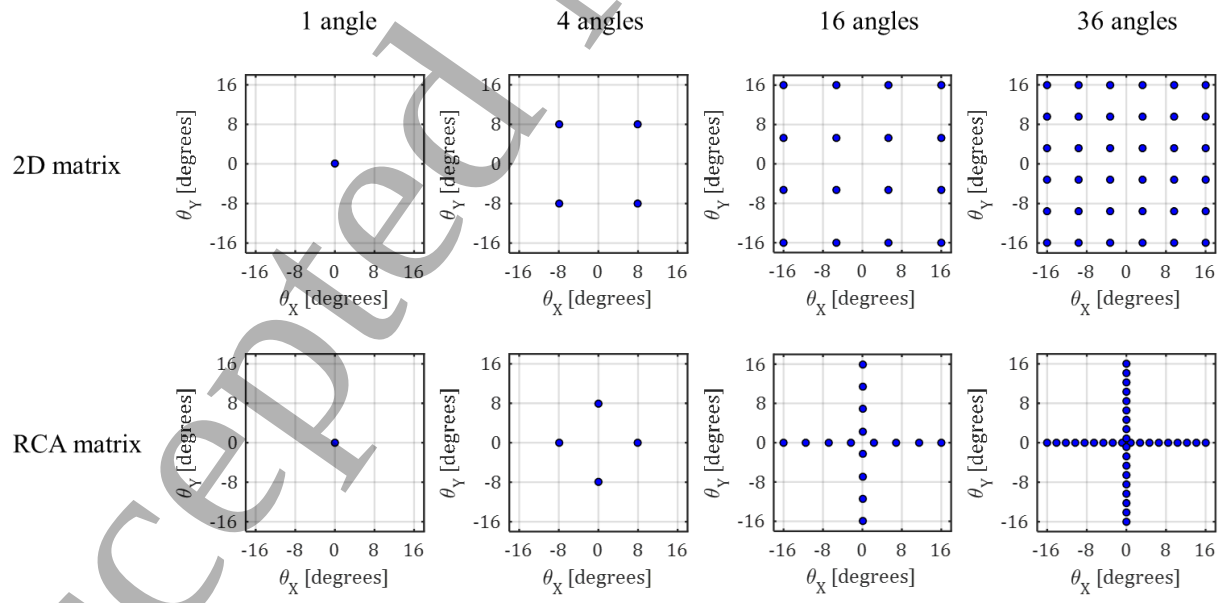

Figure 5 : Tilted plane waves represented by their angles of emission

1.7. In vitro 4D ultrafast Doppler

The experiment was performed using a custom-made Doppler phantom with ATS blood mimicking fluid passing through a 4 mm diameter vein-mimicking tube and a hydraulic pumping systems ATS 700-D 115V. The excitation of the transducer consisted of 2 periods of a 5 MHz sinusoid. This Doppler phantom was imaged using 3 sequences with different number of angle transmit: 2, 4 and 5 as shown in table 2.

Each of these sequences of 525 frames were repeated 5 times. The pulse repetition frequency was fixed at 21 KHz, therefore the volume rate was inversely proportional to the number of angle. The beamformed volume was a parallelepiped of 10 x 10 x 16 mm. Power Doppler CNR was defined as the sum of all the voxels energy included inside the real tube shape divided by the energy outside as defined by the equation (1).

	2 Angles		4 Angles				5 Angles				
θx [degrees]	-2	0	-2	2	0	0	-2	2	0	0	0
θy [degrees]	0	-2	0	0	-2	2	0	0	0	-2	2

Table 2 : Tilted plane wave angle configurations expressed in degree

1.8. In vivo 4D ultrafast Doppler

A specific sequence was developed for imaging the humeral artery of a healthy volunteer (table 3). The humeral artery was imaged using fives plane waves tilted at θ_X = [-4 4 0 0 0] and θ_Y =[0 0 0 4 4] degrees (according to the convention fixed at figure 2a). The excitation of the transducer consisted of 2 periods of a 5 MHz sinusoid. A total of 1500 compounded volumes were acquired, at a volume rate of 1.7 KHz, corresponding to an acquisition time of 0.88 second. The beamformed volume was a parallelepiped of 10 x 10 x 24 mm cube. (ISPTA = 376 mW/cm² & MI = 0.41)

Voltage	35 V
Frequency	5 MHz
Number of cycles	2
Number of tilted plane waves	5
θx, tilted plane projection on X	[-4 4 0 0 0] degrees
θy, tilted plane projection on Y	[0 0 0 -4 4] degrees
Number of compounded volumes	1500
Volume rate	1.7 KHz
Duration	0.88 s
Volume size	10 x 10 x 24 mm
ISPTA	376 mW/cm²
MI	0.41

Table 3 : In vivo sequence parameters

2. Results

2.1. PSF simulation

The simulated PSF are presented along the different planes XY (figure 6b) and XZ (figure 6c). These PSF are computed for an equal number of tilted plane wave transmitted, and thus the same volume rate of 2.9 KHz. The tilted plane wave distributions are represented in the figure 6a. The main lobe lateral width and side lobe levels are synthesized in the table 4. Since HV and VH PSF are identical with a 90° rotation, only HV is represented in the table.

	2D matrix	HV + VH	HV	
			on X	on Y
Main lobe lateral width at -6 dB [mm]	0.6	1	2	0.77
Side lobe level [dB]	-37	-16.5	-11.5	-6.75

Table 4 : PSF Main lobe lateral width and side lobe level

The PSF side lobe level associated to the 2D matrix is -37 dB while the HV + VH has a level of -16.5 dB. The lateral width at -6 dB in the 2D matrix case is 0.6 mm whereas the HV + VH has a 1 mm width.

As expected, The PSF of HV and VH are respectively elongated in the X and Y directions. In the elongated axe, the side lobe level is -11.5 dB and the lateral width is 2 mm whereas in the short axe (perpendicular to elongated axe), the side lobe level is -6.75 dB and the lateral width is 0.77 mm. The coherent summation of HV and VH allowed improving the PSF of HV and VH.

In figure 7, the PSF from the OPW sequence on RCA matrix has been computed for different set of tilted angle and thus different volume rate. The PSF quality improved rapidly with the number of plane waves up to 17. Beyond 17 angles, the PSF continues improving but at a slower rate (for this angular range configuration from -8 to +8 degrees)

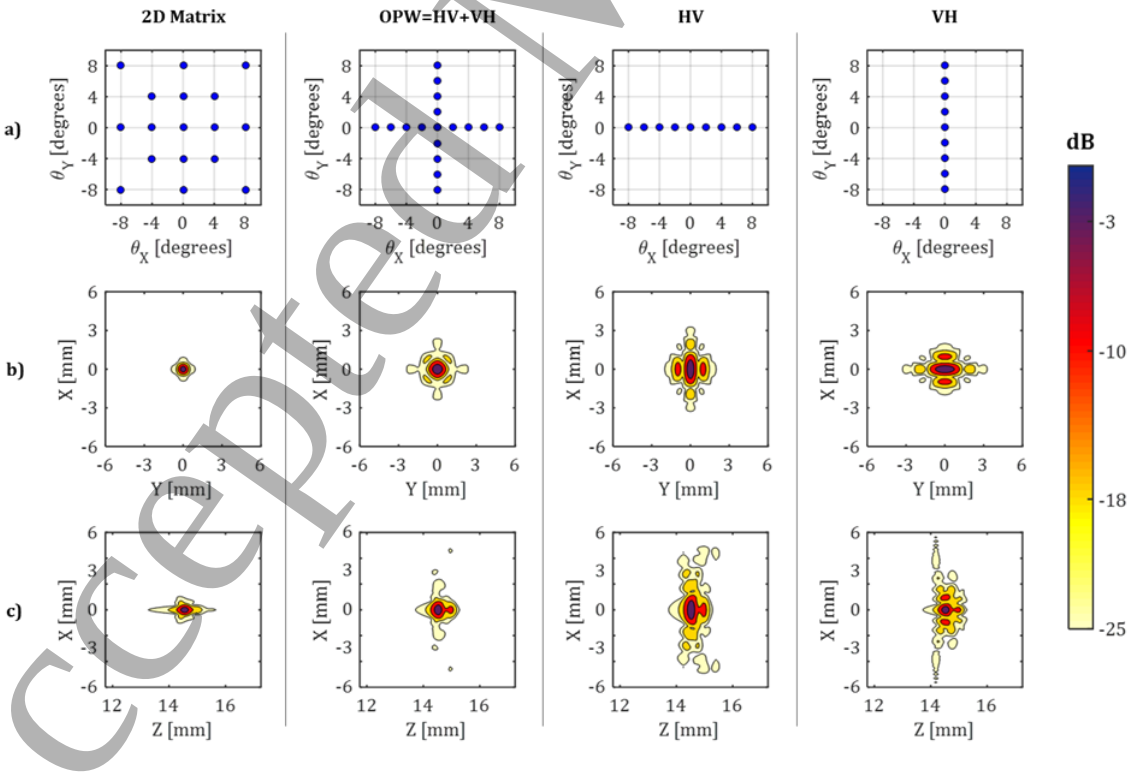

Figure 6 : Tilted plane waves represented by their angles of emission a) and theirs PSF cut view in two different planes: XY b), and XZ c), for an identical volume rate of 2.9 KHz

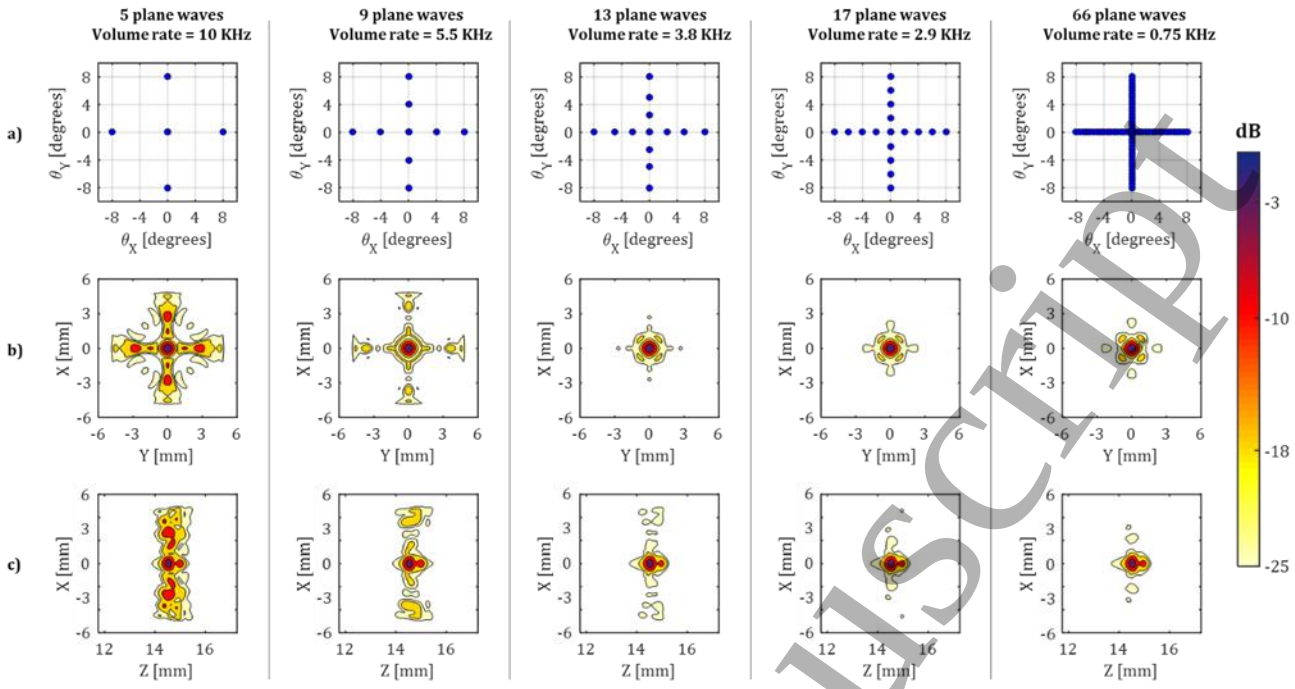

Figure 7 : Tilted plane waves represented by their angles of emission a) and RCA matrix PSF cut view in two different planes: XY b), and XZ c), for different volume rate values

2.2. In vitro 4D ultrafast CNR and resolution

Figure 8 shows RCA and 2D matrix beamformed volumes with the same frame rate, in both cases 16 plane waves were transmitted with and an angular range of -16 to +16 degrees.

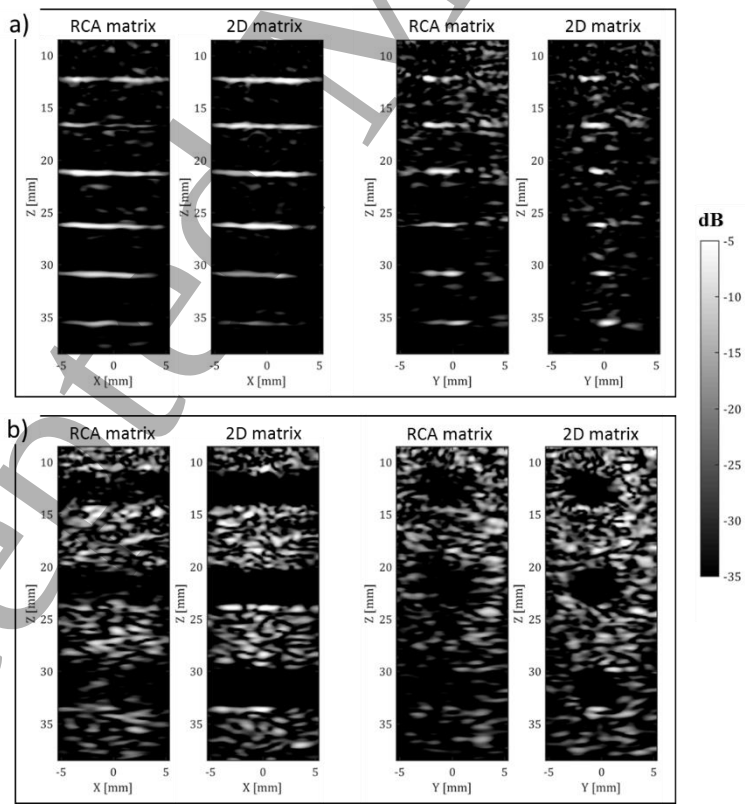

Figure 8 : 2D matrix and RCA Bscan of echogenic wires a) and anechoic cysts b)

Figure 9a shows the image CNR measured experimentally as a function of the number of transmitted plane waves for both 2D matrix (blue curve) and emulated RCA matrix (red curve) at 13 mm depth. The error bars are computed as the standard deviation over the pixel value inside the cyst. For a large number of transmits, the CNR was two times lower with the RCA than with the 2D matrix, which is consistent with the numerical simulation results.

Figure 9b, shows the lateral resolution as a function of depth for both 2D matrix (blue curve) and emulated RCA matrix (red curve) with fixed steering parameters: 16 plane waves transmitted and an angular range of -16 to +16 degrees. The lateral resolution decreased with depth and was 0.5mm with the 2D matrix and 0.6mm with the RCA.

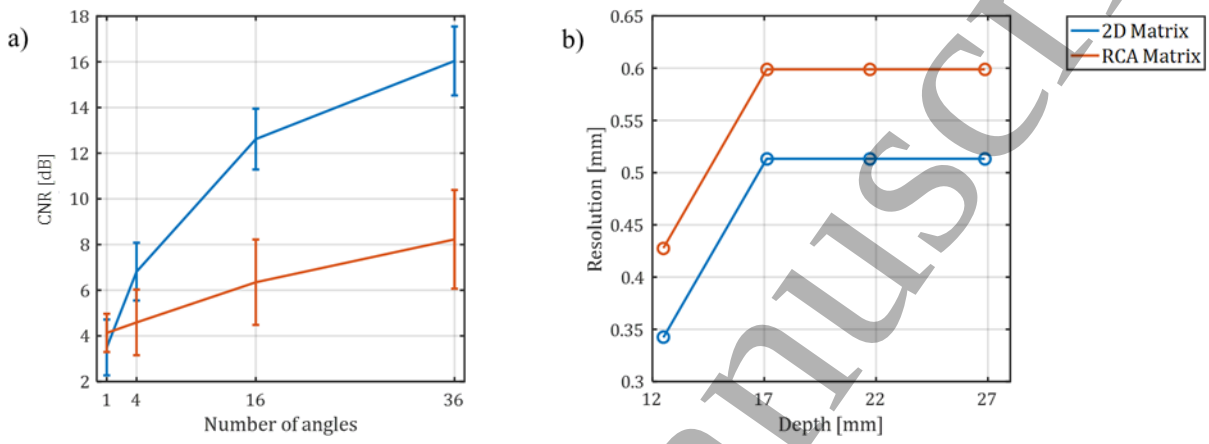

Figure 9 : CNR a) and resolution b) for both 2D matrix (blue curve) and emulated RCA matrix (red curve)

2.3. In vitro 4D ultrafast Doppler

Figure 10 shows power Doppler images presented in cross planes of the phantom flow with different number of compounded angles for the 2D matrix and the emulated RCA matrix. Transverse profile of the power Doppler are presented on figure 11. Increasing the number of compounded angles improves the power Doppler quality, which can be quantified by the power Doppler CNR. The CNR is plotted as a function of the number of angles compounded in the figure 12. The error bars on the curves correspond to the standard deviation over the five repeated experiments. Thanks to the ultrafast acquisition, a voxel based Doppler spectrum quantification can also be extracted from any voxel in the volume. The Doppler spectrum was computed as the mean of the spectrum energy from a region of interest of 6 x 6 x 6 voxels (voxel size is half lambda) centered inside the artificial vein both for the 2D matrix and the emulated RCA matrix as shown in the figure 13. The absolute errors were computed between the 2D matrix and the RCA spectrum, for each frequency and plotted on the figure 13.

These results show that in this experimental context, the power Doppler CNR with the RCA is approximately the square root of the CNR of the 2D array. Nevertheless, by increasing the number of compounded angle, RCA can achieve power Doppler with enough CNR to recover the vein shape. Regarding the Doppler spectrum, RCA gave similar frequency information but with less energy than the 2D matrix.

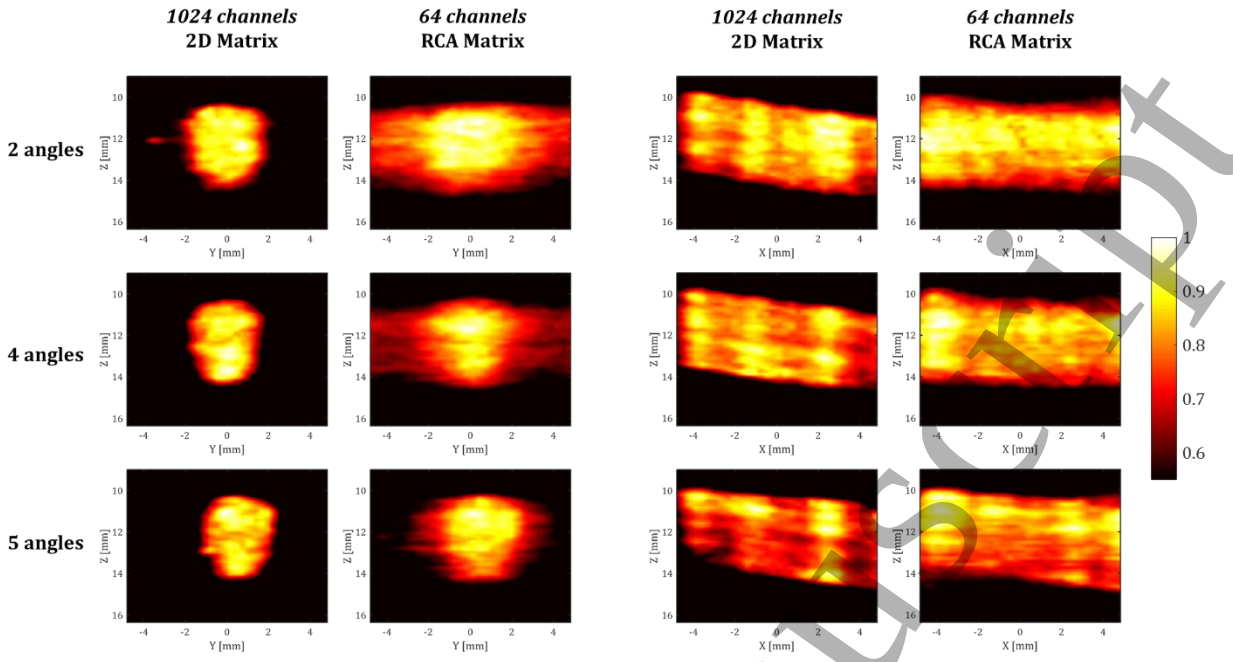

Figure 10 : Power Doppler cross views of the phantom flow with different number of compounded angles for the 2D matrix and the emulated RCA matrix

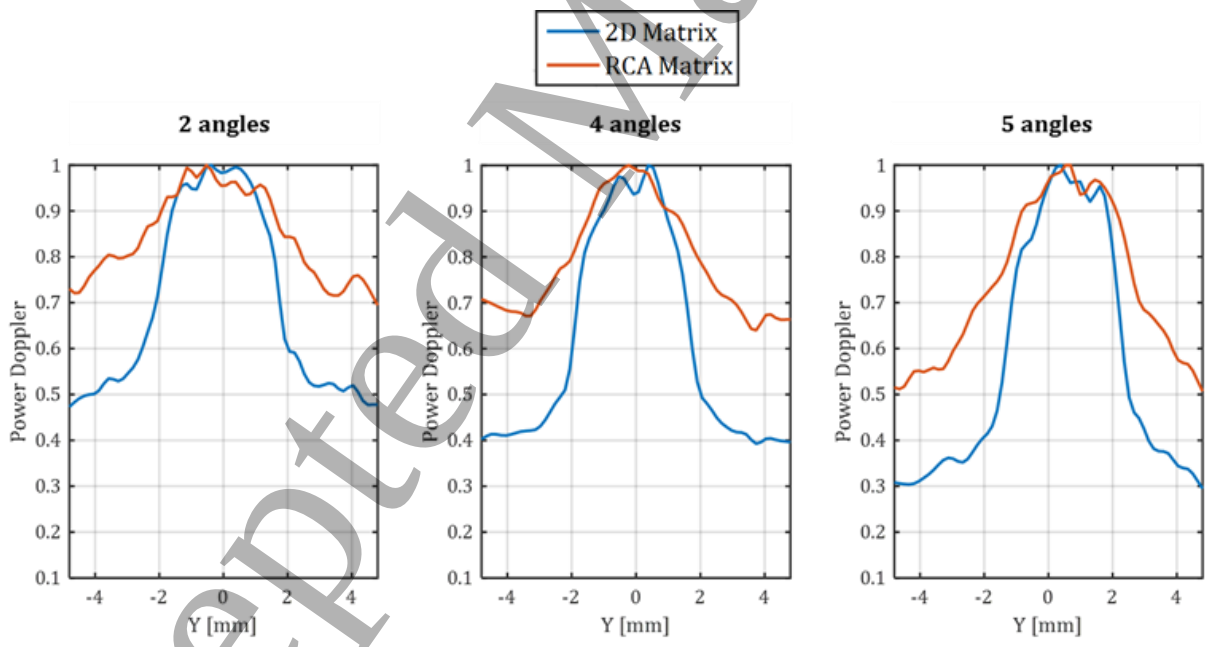

Figure 11 : Power Doppler transversal cut of the phantom flow with different number of compounded angles for the 2D matrix and the emulated RCA matrix

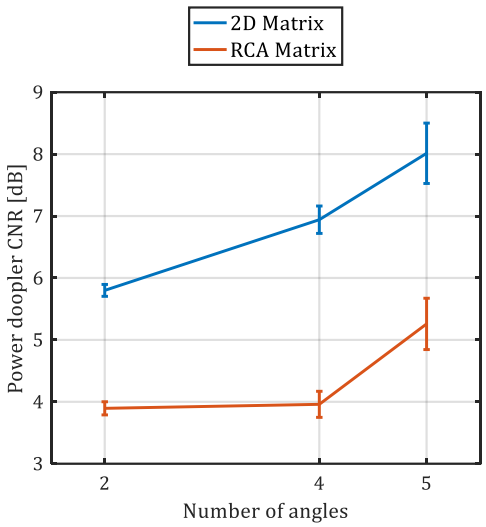

Figure 12 : Power Doppler CNR expressed in dB as a function of the numbers of compounded angles for both the 2D matrix and the emulated RCA matrix

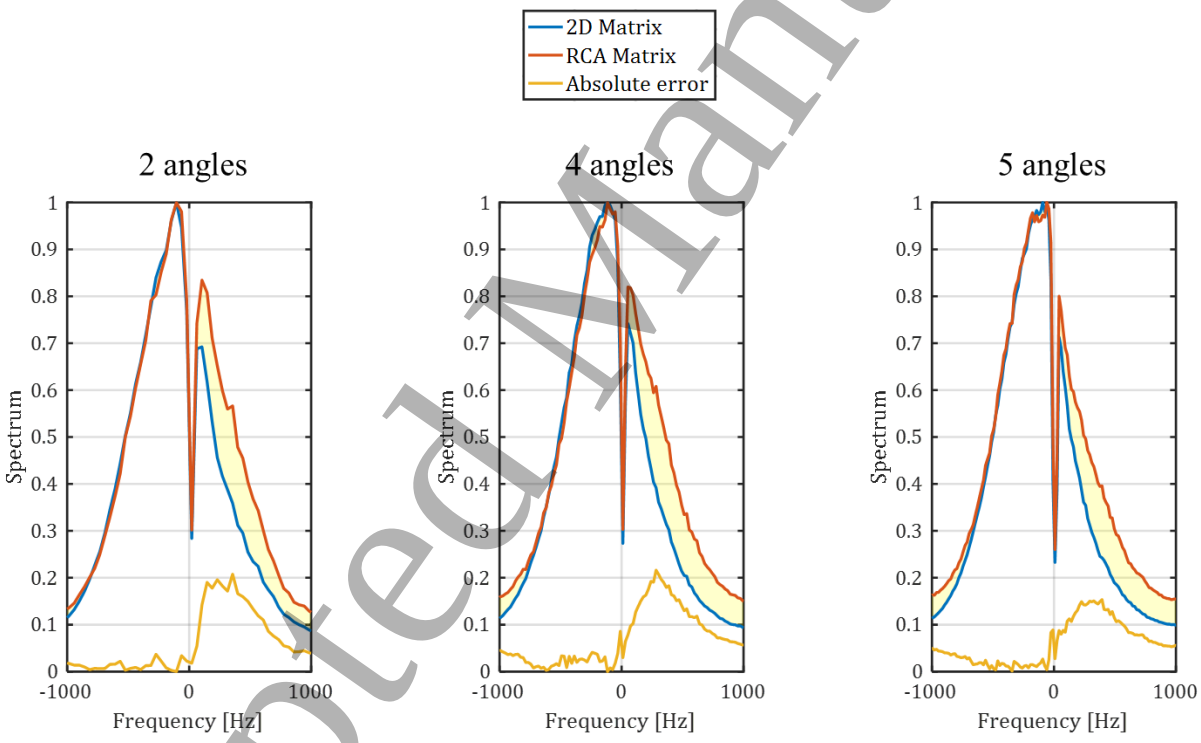

Figure 13 : Doppler spectrum of the phantom flow with different number of compounded angles for the 2D matrix and the emulated RCA matrix with their absolute errors

2.4. In vivo 4D ultrafast Doppler

For both the 2D matrix and the emulated RCA matrix, a volumetric power Doppler acquisition through different cross planes are presented in figure 14 for a human humeral artery. Power Doppler axial and transverse profiles are presented in figure 15. Thanks to the ultrafast acquisition, a voxel based pulsed wave Doppler quantification can be extracted from any voxel in the volume. We choose to non-coherently mean the spectrum from a region of interest composed of 3 x 3 x 3 voxels located in the

center of the artery for the pulsed Doppler rendering presented in the figure 16. The absolute error was computed between the RCA and the 2D matrix spectrum extracted at 0.4 and 0.6 second during respectively the systole and the diastole as shown in the figure 17.

These *in vivo* results showed that ultrafast OPW compounding imaging using emulated RCA matrix offer sufficient performances to image an artery on power Doppler and gave accurate quantification on pulsed Doppler.

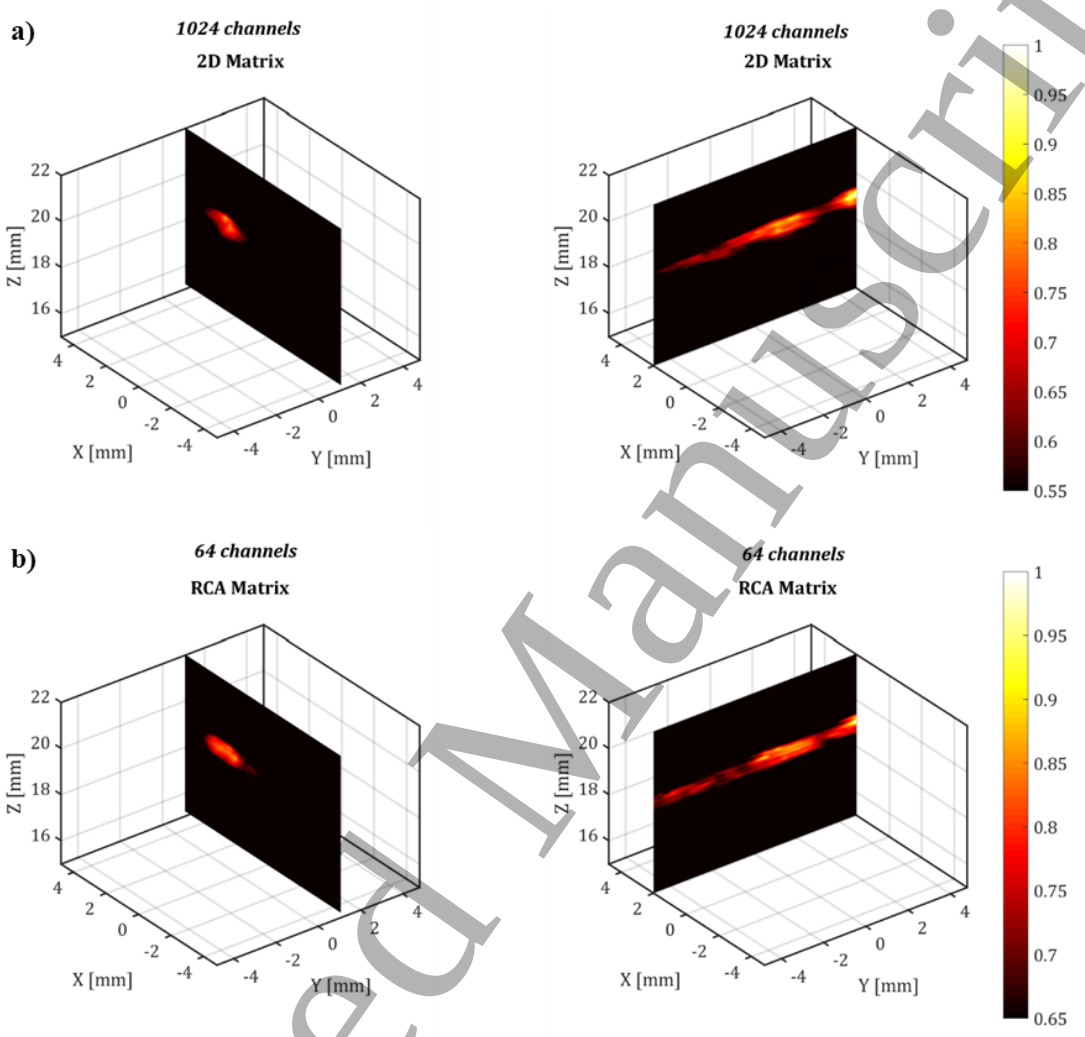

Figure 14 : In vivo power Doppler on a volunteer human humeral artery using a 2D matrix a) and an emulated RCA matrix b)

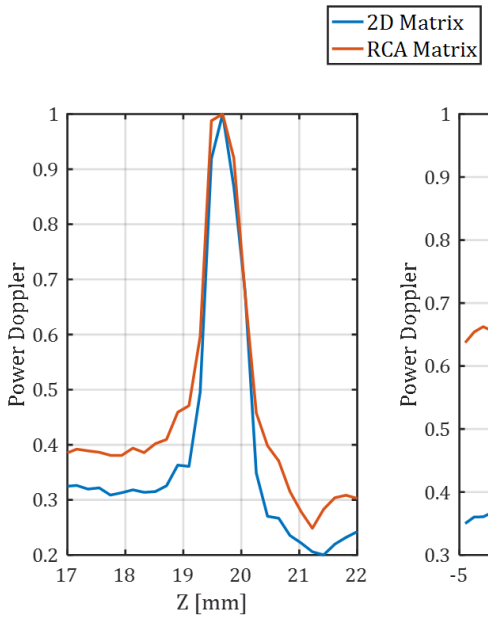

Figure 15 : Power Doppler cross cuts on a volunteer human humeral artery using a 2D matrix and an emulated RCA matrix

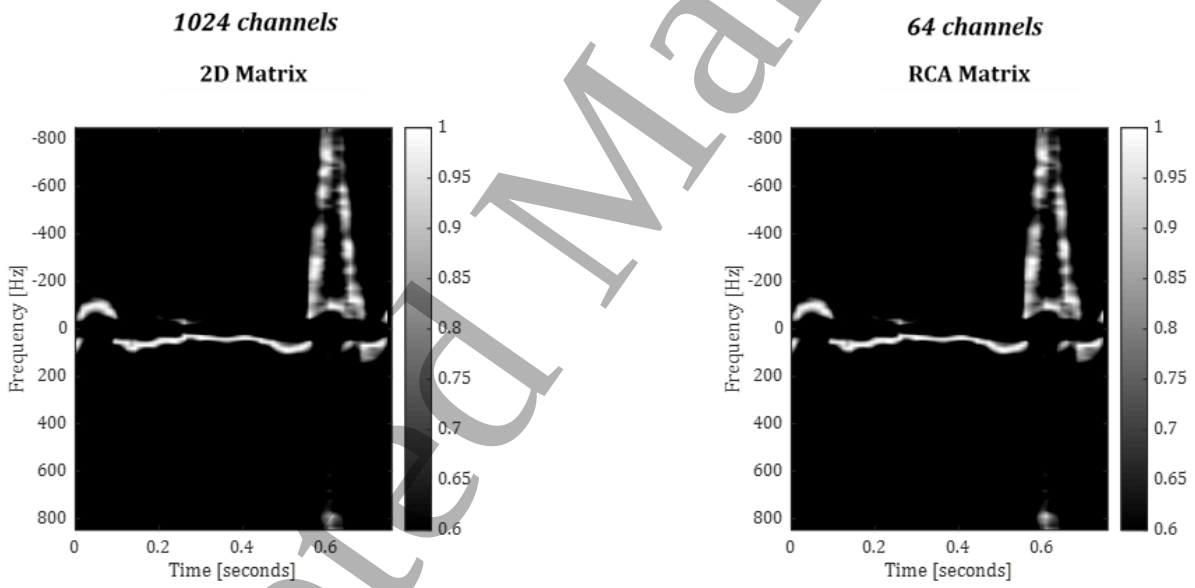

Figure 16 : In vivo pulsed Doppler on a volunteer human humeral artery using a 2D matrix and an emulated RCA matrix

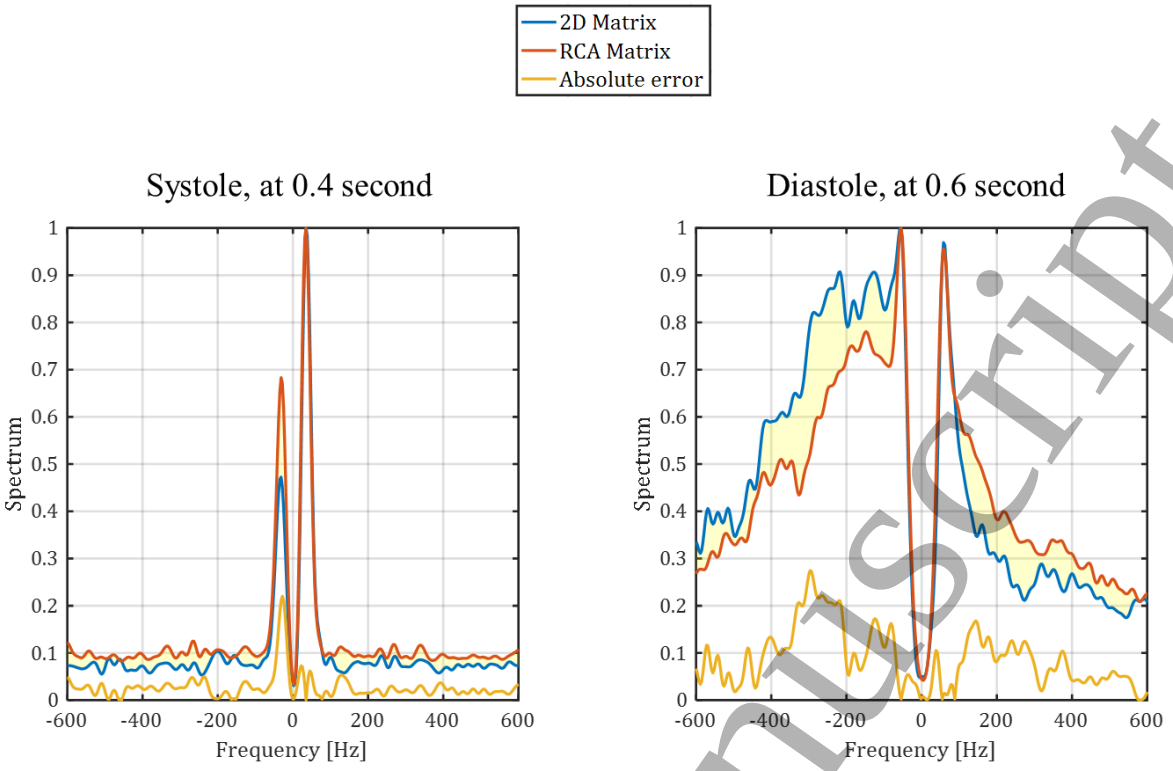

Figure 17 : In vivo pulsed Doppler extracted at 0.4 and 0.6 second for the 2D matrix, the emulated RCA and their absolute error

3. Discussion

In this paper we have investigated the performance of a RCA scheme with OPW compounding which allows the reconstruction of a large volume with only N + N channels at high volume rate. The study was deliberately focused on ultrafast Doppler imaging and comparisons with an equivalent 2D array.

Ultrafast imaging based on coherent plane wave compounding enables improving the image or volume quality by transmitting a limited number of plane waves that approximate a synthetic cylindrical focusing. In the RCA approach, however, when transmitting plane waves on one array, the symmetry between the emissions and receive focusing is broken leading to anisotropic PSF. OPW compounding was introduced in this study to compensate the anisotropy of the PSF. Jensen et al. recently published several studies describing a synthetic aperture approach for RCA matrices (Rasmussen et al. 2015). The synthetic aperture approach relied on a row-by-row element transmission with a reception of all the columns. To sweep through the whole aperture, the sequence is repeated for the *N* rows. Synthetic aperture allows the reconstruction of any kind of focusing from the acquired dataset including transmit + receive focusing and is thus very flexible. However, since the number of emissions is equal to the number of *N* elements, synthetic aperture imaging approach does not scale for high volume rate imaging, at least not for hundreds of rows but is relevant for real-time Bmode imaging.

The resolution and CNR performance of the RCA with OPW compounding were evaluated and compared to the 2D array performances. As expected, it consistently lags behind the full matrix array for a same aperture, framerate and number of emissions. As a rule of thumb, CNR of the RCA is around the square root of the 2D array (half in decibel).

Nevertheless, we have shown here the feasibility of using the RCA approach to image *in vivo* arterial blood flows in a human volunteer. Volumetric reconstruction of phantoms and a human artery vessel was performed and compared to the one obtained with the 2D matrix. An accurate Doppler spectrum was also successfully derived from these acquisitions but with less than 2D matrix sensitivity.

An important advantage of RCA arrays over 2D matrix, is the possibility to manufacture large arrays for example with more than 128 + 128 elements. A 2D matrix (128 x 128 elements) with an equivalent footprint would be too complex to manufacture and would require an electronics with very high channel count which is currently not available. A state of the art RCA array of 128 + 128 elements could therefore outperform in specific applications many of the current 2D matrix thanks to a larger aperture and/or a higher frequency.

Vector flow imaging could benefit strongly of ultrafast imaging performed with RCA arrays. Jensen et al presented initial *in vitro* results of vector flow imaging with a RCA prototype (Lehrmann et al. 2015). Correia et al showed the possibility to obtain the complete in vivo volumetric reconstruction of vector flow using ultrafast plane waves imaging with a 2D matrix (Correia et al. 2016). This work could be extended to the use of RCA arrays and would allow a simple and less expensive way to perform 4D flow imaging.

Conclusion

The RCA scheme with OPW compounding is a promising technique for 4D ultrafast Doppler imaging with a low number of acquisition channels. The imaging quality was compared to an equivalent 2D matrix with same volume rate. CNR and resolution were found to be lower than using the 2D matrix with the same volume rate. However, the CNR and resolution could be improved by adding more angles at the cost of lower volume rate. We demonstrated the feasibility of using an RCA with OPW sequence *in vivo* on human artery. OPW is a promising approach to 4D clinical vascular application with a low number of channels.

Acknowledgment

Funding for this project was provided by the French National Research Agency (ANR - DS0413 2015 -ULTRAFAST 4D)

References

Bercoff, J. et al., 2008. ShearWaveTM elastography: A new real time imaging mode for assessing quantitatively soft tissue viscoelasticity. *Proceedings - IEEE Ultrasonics Symposium*, pp.321–324.

Chen, K. et al., 2014. A column-row-parallel ultrasound imaging architecture for 3d plane-wave imaging and Tx 2nd-order harmonic distortion (HD2) reduction. *IEEE International Ultrasonics Symposium, IUS*, 1, pp.317–320.

Correia, M. et al., 2016. 4D ultrafast ultrasound flow imaging: in vivo quantification of arterial volumetric flow rate in a single heartbeat. *Physics in Medicine and Biology*, 61(23), pp.L48–L61. Available at: http://stacks.iop.org/0031-9155/61/i=23/a=L48?key=crossref.5be16dccc67ee678b4b2cd1f5eb46297.

Davidsen, R.E. & Smith, S.W., 1993. Sparse Geometries for Two-Dimensional Array Transducers in Volumetric Imaging. *IEEE Symposium on Ultrasonics, 1993*, pp.1091–1094.

Demené, C. et al., 2015. Spatiotemporal Clutter Filtering of Ultrafast Ultrasound Data Highly Increases Doppler and fUltrasound Sensitivity. *IEEE Transactions on Medical Imaging*, 34(11), pp.2271–2285.

Gennisson, J.L. et al., 2015. 4-D ultrafast shear-wave imaging. *IEEE Transactions on Ultrasonics, Ferroelectrics, and Frequency Control*, 62(6), pp.1059–1065.

Hara, K. et al., 2005. A New 80V 32x32ch Low Loss Multiplexer LSI for a 3D Ultrasound Imaging System. *Power Semiconductor Devices and ICs, 2005. Proceedings. ISPSD '05. The 17th International Symposium on*, pp.359–362.

Jensen, A. & Svendsen, B., 1992. Calculation of Pressure Fields from Arbitrarily. *Ultrasonics, Ferroelectrics and Frequency Control, IEEE Transactions*, 39(2), pp.262–267.

Jensen, J.A. et al., 2013. SARUS: A synthetic aperture real-time ultrasound system. *IEEE Transactions on Ultrasonics, Ferroelectrics, and Frequency Control*, 60(9), pp.1838–1852.

Lehrmann, T. et al., 2015. 3-D Vector Velocity Estimation with Row-Column Addressed Arrays. *Proceedings of IEEE International Ultrasonics Symposium*, 3010(c).

Logan, A.S., Wong, L.L. & Yeow, J.T.W., 2009. 2-D CMUT wafer bonded imaging arrays with a row-column addressing scheme. *Proceedings - IEEE Ultrasonics Symposium*, pp.984–987.

Mace, E. et al., 2013. Functional ultrasound imaging of the brain: Theory and basic principles. *IEEE Transactions on Ultrasonics, Ferroelectrics, and Frequency Control*, 60(3), pp.492–506.

Montaldo, G. et al., 2009. Coherent plane-wave compounding for very high frame rate ultrasonography and transient elastography. *IEEE Transactions on Ultrasonics, Ferroelectrics, and Frequency Control*, 56(3), pp.489–506.

Morton, C.E.C.E. & Lockwood, G.R.G.R., 2003. Theoretical assessment of a crossed electrode 2-D array for 3-D imaging. *IEEE Symposium on Ultrasonics, 2003*, 1(c), pp.968–971. Available at: http://ieeexplore.ieee.org/lpdocs/epic03/wrapper.htm?arnumber=1293560.

Provost, J. et al., 2015. 3-D ultrafast doppler imaging applied to the noninvasive mapping of blood vessels in Vivo. *IEEE Transactions on Ultrasonics, Ferroelectrics, and Frequency Control*, 62(8), pp.1467–1472.

Provost, J. et al., 2014. 3D ultrafast ultrasound imaging in vivo. *Physics in medicine and biology*, 59(19), pp.L1–L13. Available at: http://www.pubmedcentral.nih.gov/articlerender.fcgi?artid=4820600&tool=pmcentrez&rendertype=abstract.

Rasmussen, M.F. et al., 2015. 3-D imaging using row-column-addressed arrays with integrated apodization -Part i: Apodization design and line element beamforming. *IEEE Transactions on Ultrasonics, Ferroelectrics, and Frequency Control*, 62(5), pp.947–958.

Ratsimandresey, L. et al., 2002. A 3 MHz two dimensional array based on piezocomposite for medical imaging. *2002 IEEE Ultrasonics Symposium, 2002. Proceedings.*, 2(c), pp.1265–1268. Available at: http://ieeexplore.ieee.org/lpdocs/epic03/wrapper.htm?arnumber=1192524.

Savord, B. & Solomon, R., 2003. Fully sampled matrix transducer for real time 3D ultrasonic imaging. *IEEE Symposium on Ultrasonics, 2003*, 1(c), pp.945–953.

Seo, C.H. & Yen, J.T., 2009. A 256 x 256 2-D array transducer with row-column addressing for 3-D rectilinear imaging. *IEEE Transactions on Ultrasonics, Ferroelectrics, and Frequency Control*, 56(4), pp.837–847.

Tanter, M. & Fink, M., 2014. Ultrafast imaging in biomedical ultrasound. *IEEE Transactions on Ultrasonics, Ferroelectrics, and Frequency Control*, 61(1), pp.102–119.

Tiran, E. et al., 2015. Multiplane wave imaging increases signal-to-noise ratio in ultrafast ultrasound imaging. *Physics in Medicine and Biology*, 60(21), pp.8549–8566. Available at: http://stacks.iop.org/0031-9155/60/i=21/a=8549?key=crossref.0af5c4f84e9506dfd5a70e4eb26df274.

Yen, J.T. et al., 2009. A dual-layer transducer array for 3-D rectilinear imaging. *IEEE Transactions on Ultrasonics, Ferroelectrics, and Frequency Control*, 56(1), pp.204–212.